Results in Engineering 3 (2019) 100032

Contents lists available at ScienceDirect

Results in Engineering

journal homepage: www.editorialmanager.com/rineng/Default.aspx

Hazard risks pertaining to partially submerged non-stationary vehicle on low-lying roadways under subcritical flows

Syed Muzzamil Hussain Shah [a,*], Zahiraniza Mustaffa [a], Eduardo Matínez-Gomariz [b], Khamaruzaman Wan Yusof [a], Ebrahim Hamid Hussein Al-Qadami [a]

[a] Department of Civil and Environmental Engineering, Universiti Teknologi PETRONAS, 32610, Seri Iskandar, Perak, Malaysia
[b] Flumen Research Institute, Technical University of Catalonia, Barcelona, Spain

ARTICLE INFO

Keywords:
Hydrodynamic forces
Non-stationary vehicle
Low-lying roadway
Subcritical flows
Partial submergence

ABSTRACT

Rivers overflowing onto the floodplains can seriously disrupt the transportation system which can cause significant risks to moving or parked vehicles. The major flooding occurrence at the East Coast of Malaysia in December 2014 for instance, exhibited several hazards and fatalities involving vehicle submergence when the road conditions at low-lying flooded roadways were not known to the road users. To imitate a similar situation, the hydraulic characteristics of river overtopping an adjacent low-lying roadway during floods and the dynamics response of a vehicle attempting to cross over such flows were carried out in a modelled experimental set up. With that regards, a Perodua Viva which represents the medium-sized Malaysian passenger car was manufactured (1:10), ensuring similarity laws. Further, to monitor significant threats a flooded vehicle could face, the low-lying roadway model was designed to the allowable grade of five percent as proposed in Arahan Teknik (Jalan), ATJ 8/86. Keeping in view the height of the car and subcritical state of the flow, the range of water depths between 0.047 and 0.089 m, whereas for velocities, it was controlled to be in between 0.20 and 0.39 m/s, respectively. The buoyancy depth was noticed at depths greater than and equal to 0.055 m. Below critical depth, mode of sliding failure relied on the dominancy of varying horizontal pushing forces, namely frictional resistance, rolling friction, drag and driving forces.

Introduction

Globally, flooding is the most common and most costly natural hazard [1–3]. Among public infrastructures, the transportation systems are often highly exposed to flood risk due to their considerable size [4,5]. Flood fatality data show that worldwide, flood related deaths are increasingly associated with people perishing in vehicles that become unstable while driving through floodwaters [6–9]. On the subject of flood hazards relating to vehicle movement, rivers overflowing onto the floodplains can seriously disrupt the transportation system by cutting off the roads and railway networks, as well as leading to significant risks to vehicles that are moving or parked along floodplains [10]. At times, the intensity of flood flows could wash away the flooded vehicles which could damage the infrastructure or even cause loss of human life through collision [11,12]. It is therefore vital to investigate the hydraulic behavior and hazard conditions of vehicles to reduce or ideally minimize such possible disastrous consequences [13,14]. An analysis of flood rescue data shows that occupied vehicles that become unstable due to the force of floodwaters are vulnerable to being washed off roadways and bridges into even deeper, more dangerous flows [15]. Unfortunately, many flood-related drowning fatalities are caused by individuals intentionally driving the motor vehicles into low-lying flooded waterways which is the leading cause of floodwater related drowning deaths [9].

Studies on vehicle instability in floodwaters initiated when several incidents concerning cars floating away from the causeways were reported in New South Wales in February 1967. Bonham and Hattersley (1967), being the pioneers, initiated the experimental investigations on a scaled vehicle by determining the effects of vertical and horizontal reaction forces on a parked vehicle positioned perpendicular to a flooded crossing [16]. A similar empirical approach was undertaken by Gordan and Stone (1973) on a scaled vehicle at different braking conditions. In the given, the vehicle was positional parallel to the incoming flow direction all the times [17]. Outcomes from both studies developed the limits of friction coefficients between the road surface and the vehicle tires. Later, a theoretical approach following the mechanical condition of sliding equilibrium to determine the incipient velocity for a flooded

* Corresponding author.
E-mail address: syed.muzzamil_g03359@utp.edu.my (S.M.H. Shah).

https://doi.org/10.1016/j.rineng.2019.100032
Received 18 May 2019; Received in revised form 6 July 2019; Accepted 8 July 2019

vehicle was proposed by Keller and Mitsch (1993) [18]. All these studies involved medium-sized conventional cars commonly found on road sides during that era. However, the modern motor vehicles have undergone several gradual enhancements over time, specifically in terms of aerodynamic design, ground clearance, sealing capacity and vehicle weight (lightweight metal chassis). Thus, it has been argued that the results of those former studies (1967–1993) may no longer be appropriate for modern cars and cannot be adopted permanently.

It has been expressed that after the theoretical analyses proposed by Keller and Mitsch (1993), no significant work in the vicinity of vehicle stability in floodwaters was published until 2010. Therefore, the existing safety guidelines (Australian Rainfall and Runoff, AR&R - 2011) on vehicle stability in floodwaters are based on the study outcomes proposed during the earlier inquiries and does not include the results of subsequent studies (2010–2017) published very close or after its release.

Teo et al. (2010) and Xia et al. (2010) performed their studies on the same line of research by assessing the instability failure modes of variety of static modern cars at the University of Cardiff [19,20]. Xia et al. (2010) proposed a detailed formulation to predict the incipient velocity of flooded vehicles based on the mechanical condition of sliding equilibrium which was later validated through the experimental results of Teo et al. (2010), for the three-tested scaled model vehicles (1:43). Note that herein only the rear end of the vehicle facing the incoming flow direction was considered. Later, Shu et al. (2011) derived a semi-empirical formula for critical motion conditions for partly submerged cars (front and rear ends of the vehicle). The formula offered a new approach where the buoyancy depth was considered to highlight floating depths for static vehicles. This critical depth was not applicable to the cars tested by Teo et al. (2010) mainly due to density concerns. However, the experimental runs performed by Shu et al. (2011) ensured Froude similarity in all aspects, namely density, adapted weight and scale ratios [21]. Other experimental investigations were performed by Toda et al. (2013). By far, it is only study of its kind where a new approach was adopted by taking into consideration, the void space rate and the additional mass, namely passengers and luggage weight, inside a car [22]. A variation of the Shu et al. (2011) formula was proposed by Xia et al. (2013) by considering the incoming flow direction relative to the vehicle length (the vehicle side end only) [23] and lastly, Martínez-Gomariz et al. (2017) suggested a novel approach to assess the stability thresholds for any real static car exposed to floodwaters. This study also involved the analysis of both buoyancy and friction effects [24].

From the reported works, it seemed that almost all investigations were merely dedicated to static (parked) vehicles. Due to the complexity of the stability analysis for non-static cars attempting to cross flooded streets, the instability failure mechanism for such circumstances is still not well understood.

In the current investigation, an attempt has been made to study the behaviour of a non-stationary (in motion) vehicle towards the varying combinations of incoming flow velocity (v) and water depth (y). Note that the study was limited to direction of incoming flow perpendicular to the vehicle movement. Contrary to previous studies performed on static (parked) vehicles, the innovation herein appears when the influence of rolling friction due to tires rotation and the contribution of driving force which imposes another unique force, namely acceleration, were considered. Moreover, the impact of weight components due to slope inclination gave additional exposure to the instability failure mechanism.

Methodology

Investigations on the non-static vehicle were performed in a water retaining structure ($5 \times 4.25\ m^2$), located at the hydraulics laboratory, Universiti Teknologi PETRONAS (UTP), Malaysia. A hanging bridge connected to the ceiling was used throughout the investigations to avoid direct contact of floodwater while computing the hydraulic variables. The measurement tools such as point gauge, current meter, line laser and camcorder were placed on the moveable hanging bridge itself. The depth and velocity measurements were recorded at one vehicle length upstream of the flooded vehicle [20]. Herein a Perodua Viva which represents the medium-sized Malaysian passenger car was manufactured (1:10), ensuring similarity laws. Further, the tires of the model were made from the same material as of the prototype, *i.e.*, natural and synthetic rubber, fabric and wire along with carbon black and other chemical compounds. Thus, ensuring that the similarity law of the friction coefficient was also met. The specifications of the model and prototype are shown in Table 1. Vehicle instability was computed at varying discharges and water depths. Further, the driving force was assessed by recording the time taken by the vehicle to reach a known distance. The scope of the study being partial submergence, thus water depths were set in close resemblance to the limits allowed for the vehicle height. Moreover, the range of flow velocities and water depths ensured the flow to be in subcritical state all the times. Following similar steps, the experimental data was collected for several flow and depth combinations. The description and the side view diagram of the experimental setup are shown in Figs. 1 and 2, respectively.

Table 1
Vehicle specifications.

Vehicle	Scale	Length (mm)	Width (mm)	Height (mm)	Kerb weight (g)
Perodua Viva	Prototype Model (1:10)	3575 357.5	1475 147.5	1530 153.0	≈800000 880

Fig. 1. Laboratory investigations performed at the hydraulics laboratory, UTP.

Laboratory investigations

The hydrodynamic response of the vehicle towards instability failure mode at varying hydraulic variables were computed. The values for Froude and Reynolds number attained during the experimental investigations are shown in Table 2. From the table, it can be inferred that the value of Froude number remained less than 1 always which ensures that the state of the flow was subcritical. Further, the minimum value of Reynolds number was found to be in order of 16000. Flows in the flumes can be categorized as free surface flow which are generally driven both by gravity and inertia. Therefore, Froude number is the best correlation required to analyze the flow. Conversely, Reynolds number deals with the relationship between frictional and inertial forces. For various reasons, the requirements posed by both Froude and Reynolds numbers cannot be concurrently satisfied. Typically, free surface flows are governed by gravity forces, whereas Reynolds number effects (viscous drag) are most likely to become more significant at lower Reynolds number.

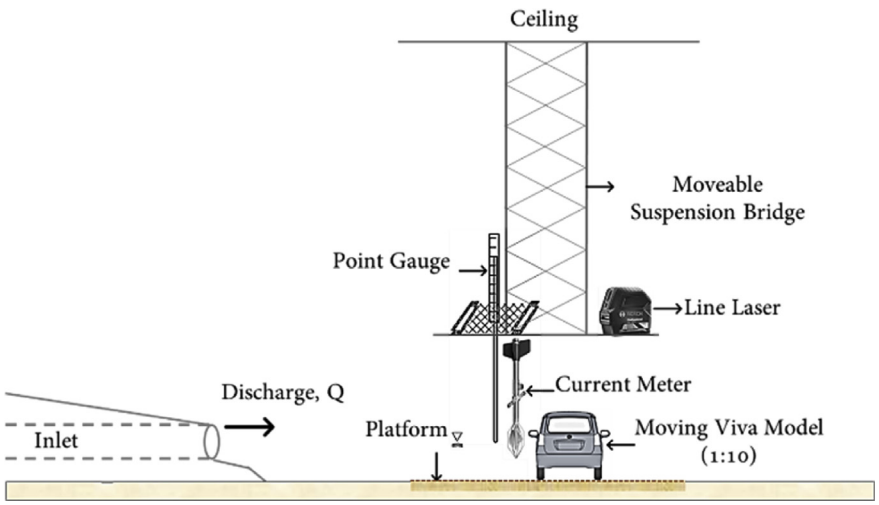

Fig. 2. Side view of experimental setup.

Table 2
Froude and Reynolds number.

No.	Velocity (m/s)	Depth (m)	Froude Number	Reynolds Number
1.	0.39	0.047	0.57	18330
2.	0.29	0.059	0.38	17110
3.	0.28	0.065	0.35	18200
4.	0.24	0.077	0.28	18480
5.	0.22	0.083	0.24	18260
6.	0.20	0.089	0.21	17800
7.	0.29	0.057	0.39	16530
8.	0.29	0.060	0.38	17400
9.	0.26	0.071	0.31	18460
10.	0.24	0.078	0.27	18720
11.	0.20	0.087	0.22	17400
12.	0.32	0.055	0.44	17600
13.	0.28	0.061	0.36	17080
14.	0.26	0.072	0.31	18720
15.	0.24	0.079	0.27	18960
16.	0.20	0.088	0.22	17600

From Fig. 3, it can be seen that when the water depth was greater than and equal to 0.055 m, floating instability occurred which mainly happened due to the buoyancy force that surpassed the vehicle weight. The buoyancy force concerns to the submerged fractions of the car, *i.e.*, volume only, therefore at mild inclination, higher water depths were required to cause floating failure. Conversely, below critical depth, sliding failure was noticed slightly at lower depths and high flows. The mainly happened because at lower depths, the buoyancy force was insufficient to cause floating instability failure. Further, the incipient velocity needed to slide a vehicle decreased with an increase in the ground slope.

Numerical approach

The impact of buoyancy and lift forces to cause a vehicle to float in floodwaters varies based on the transition between the flow states *i.e.* subcritical and supercritical flow conditions. For instance, the impact of buoyancy force can be neglected for high flow velocities, thereby considering only the effect of lift force [24], whereas for subcritical flows, the contribution of lift force has been reported insignificant [25,26]. Therefore, herein the impact of lift force has not been taken into consideration for further analysis. However, the following section reports on the forces, namely buoyancy force (F_B), drag force (F_D), frictional resistance (F_R), rolling friction (F_{RO}) and driving force (F_{DV}) determined for a partially submerged vehicle attempting to cross a low-lying flooded roadway. On a flat road condition, the normal reaction force F_N is equal to vehicle weight F_G as the ground slope remains at zero degree as shown in Fig. 4. However, when the surface gradient is at an angle, the gravitational force has transverse components, namely $mgy = mg\cos\theta$ and $mgx = mg\sin\theta$ as shown in Fig. 5. These weight components affect the vehicle weight and so does the instability modes [19].

In the preceding studies related to stationary flooded vehicles, the value of friction coefficient was set to a constant value of 0.3, as proposed by Bonham and Hattersley (1967) [16]. Herein the friction coefficients both for frictional resistance (μ) and rolling resistance (μ_{RO}) were experimentally determined. On the other hand, the value of drag coefficient (C_D) was selected based on the given range of Reynolds number. It is important to emphasize that in case of non-stationary vehicles attempting to cross flooded streets where the flow direction is perpendicular to the vehicle movement, then the drag force by the flood flow usually impacts at two directions, namely perpendicular to vehicle movement (D_1) and parallel and opposite to the driving force (D_2).

Buoyancy force

The buoyant force exerted on a body immersed in a fluid is equal to the weight of the fluid the body displaces. Herein the floodwater depth was estimated at the point of maximum inclination for the computation of buoyancy force. With that regards, the vehicle chassis and tires were precisely designed in AutoCAD. These parts were later enhanced to a three-dimensional model through SolidWorks. Lastly, the submerged volume of the vehicle was attained by using ANSYS (Static Structural) as shown in Fig. 6. It is important to emphasize that the vehicle chassis and tire were separately designed and assessed because at several water depths only the front wheels and some of the front bumper area were covered. However, to attain the submerged volume under such conditions some modifications were made to the platform so that proper estimation of submerged dimensions can be ensured. The submerged fractions attained from the vehicle chassis and tires were later accumulated to get the total submerged volume (V) of the immersed car.

Depending on the level of vehicle submergence, the submerged volume of the chassis and the tires were accumulated for the computation of buoyancy force is highlighted in Table 3.

From Table 3, it can be seen that as water depth increased, the impact of buoyancy force on the vehicle also increased mainly because of immersion. However, it can be noticed that the maximum buoyancy force was observed, *i.e.,* 23.93 N, when the floodwater level reached 0.089 m, whereas its impact was found low, *i.e.,* 5.99 N, when the water level was at 0.047 m.

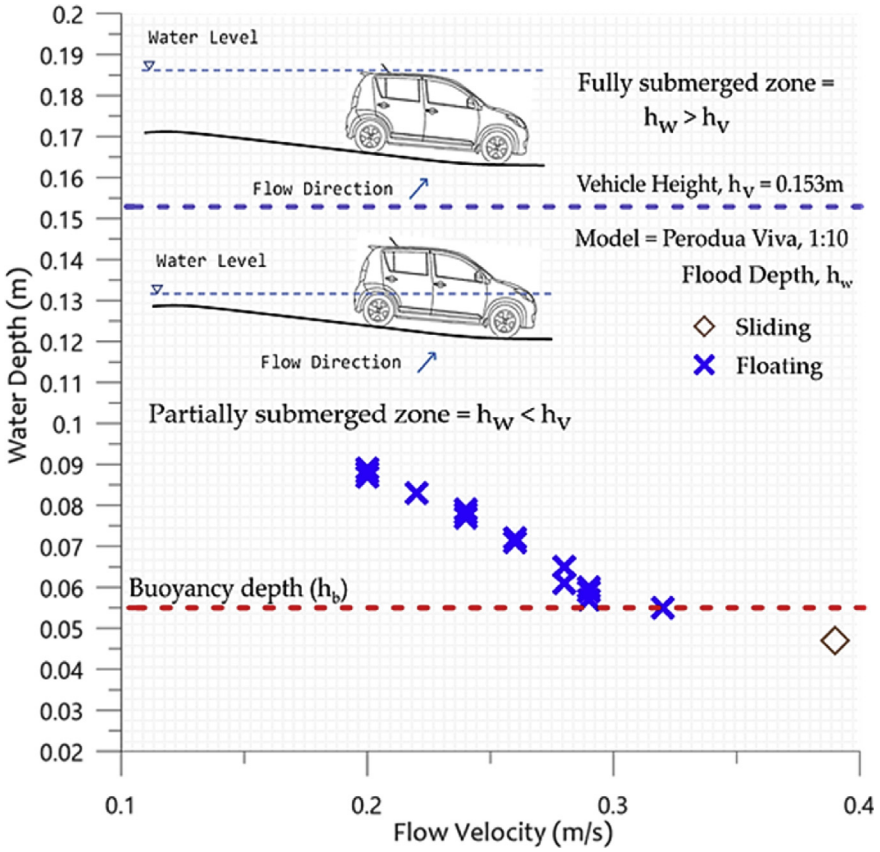

Fig. 3. Instability thresholds assessed through laboratory investigations.

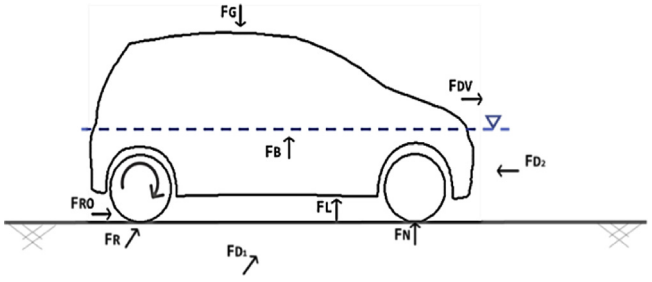

Fig. 4. Hydrodynamic forces on a non-stationary vehicle in floodwaters.

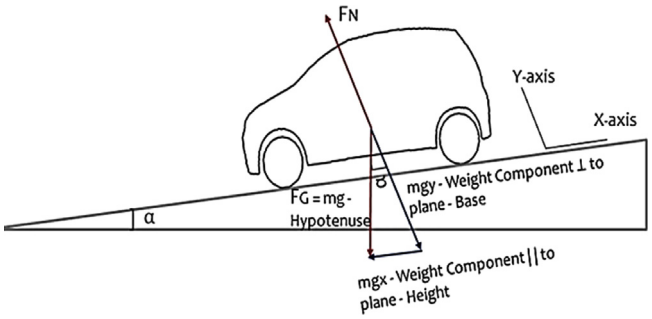

Fig. 5. Weight components distribution when the ground slope is at an angle.

Drag force

As mentioned earlier, when the surface gradient is at an angle, the gravitational force has transverse components. The parallel component, namely $mgx = F_G sin\theta$, assists the drag force to cause sliding failure. Thus, when the vehicle is in floodwaters where the state of the flow remains subcritical, then the parallel component of the force becomes, $mgx = (W - F_B)\sin\theta$. Therefore, the overall impact of drag force to cause sliding failure at inclinations is equivalent to $\frac{1}{2}\rho C_D A_D v^2 + (W - Fb)\sin\theta$. Hence, it can be said that at inclinations, the impact of drag force to cause sliding failure increases. Concerning drag force, the minimum value of Reynolds number was found to be in the order of 16000, therefore, the value drag coefficient remained unchanged and was set to a constant value based on the level of the water depth with respect to the chassis height [20,27]. The influence of drag force at the side end of the vehicle (D_1, perpendicular to the flow direction) is presented in Table 4. On the other hand, its impact at the front end (D_2, parallel and opposite to the driving force) was also assessed and was found to be insignificant. Thus, it has been disregarded in this study from further consideration.

Table 4 highlights the impact of drag force at the side end of the vehicle (D_1). Compared to the buoyancy force as discussed in the former section, it can be noticed that the magnitude of drag force did not necessarily increase with an increase in the water depth. This happened because the drag force does not rely alone on the flood depth and it usually varies based on the varying hydraulic variables, *i.e.,* flood depth and velocity. For instance, at 0.087 m and 0.02 m/s, the impact of drag force was found to be 0.44 N. On the other hand, at 0.047 m and 0.38 m/s, its impact was found to be 0.56 N.

Friction force

At inclined platforms, the frictional resistance of the tire with the ground surface further reduces due to perpendicular component of the gravitational force. For instance, on a flat surface, the friction force is equivalent to μF_N, however, at inclination this force is transformed into $\mu F_N(cos\theta)$. Herein the friction coefficients (wet surface) were experi-

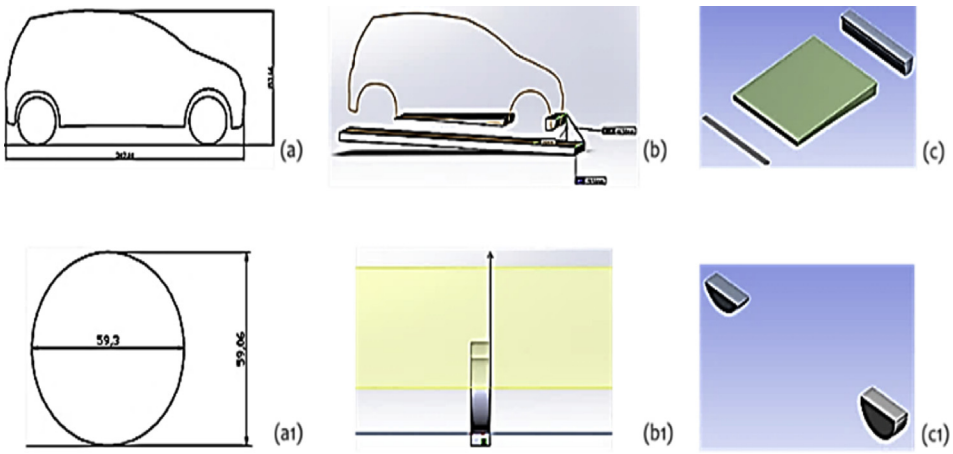

Fig. 6. Estimation of vehicle's submerged fractions (a, a_1) AutoCAD, (b, b_1) SolidWorks and (c, c_1) ANSYS (Static Structural).

Table 3
Computation of buoyancy force through AutoCAD, SolidWorks and ANSYS (Static Structural.

No.	Depth (m)	Submerged Volume, Chassis only (m^3)	Tyres Volume (m^3), Depending on the Level of Submergence	Buoyancy Force (N)
1.	0.047	0.00047	0.00014	5.99
2.	0.059	0.00088	0.00019	10.46
3.	0.065	0.00110	0.00020	12.79
4.	0.077	0.00163	0.00022	18.07
5.	0.083	0.00193	0.00022	21.02
6.	0.089	0.00222	0.00022	23.93
7.	0.057	0.00081	0.00018	9.70
8.	0.060	0.00091	0.00019	10.84
9.	0.071	0.00135	0.00021	15.35
10.	0.078	0.00167	0.00022	18.55
11.	0.087	0.00213	0.00022	22.97
12.	0.055	0.00071	0.00018	8.72
13.	0.061	0.00095	0.00020	11.23
14.	0.072	0.00140	0.00022	15.80
15.	0.079	0.00173	0.00022	19.05
16.	0.088	0.00217	0.00022	23.45

Table 4
Drag impact at vehicle's side end, D_1.

No.	Water Depth, (m)	Flow Velocity, v^2 (m/s)	Submerged Area Projected Normal to the Flow, A (m^2)	Drag Force, F_{D1} (N)
1.	0.047	0.15	0.00674	0.56
2.	0.059	0.08	0.01069	0.49
3.	0.065	0.08	0.01257	0.54
4.	0.077	0.06	0.01648	0.52
5.	0.083	0.05	0.01852	0.49
6.	0.089	0.04	0.02053	0.45
7.	0.057	0.08	0.01004	0.46
8.	0.060	0.08	0.01101	0.51
9.	0.071	0.07	0.01451	0.54
10.	0.078	0.06	0.01681	0.53
11.	0.087	0.04	0.01987	0.44
12.	0.055	0.10	0.00923	0.52
13.	0.061	0.08	0.01133	0.49
14.	0.072	0.07	0.01485	0.55
15.	0.079	0.06	0.01716	0.54
16.	0.088	0.04	0.02020	0.44

mentally determined both for (F_R) and (F_{RO}) through the spring balance approach. The value of friction coefficient for the assessment of frictional resistance was noticed to be 0.19, whereas for the rolling friction, the coefficient was found to be 0.048. The values (F_R) and (F_{RO}) attained at varying hydraulic variables are shown in Table 5.

Table 5
Friction force both (F_R) and (F_{RO}).

No.	Effective Weight, N (Cosθ) (N)	Rolling Friction Force, F_{RO} (N)	Friction Force, F_R (N)
1.	2.63	0.13	0.50
2.	−1.83	−0.09	−0.35
3.	−4.15	−0.20	−0.79
4.	−9.43	−0.45	−1.79
5.	−12.36	−0.59	−2.35
6.	−15.27	−0.73	−2.90
7.	−1.07	−0.05	−0.20
8.	−2.21	−0.11	−0.42
9.	−6.70	−0.32	−1.27
10.	−9.90	−0.48	−1.88
11.	−14.31	−0.69	−2.72
12.	−0.09	0.00	−0.02
13.	−2.59	−0.12	−0.49
14.	−7.15	−0.34	−1.36
15.	−10.40	−0.50	−1.98
16.	−14.79	−0.71	−2.81

Table 6
Driving force.

No.	Vehicle Velocity (m/s), V_1	Vehicle Velocity (m/s), V_2	Vehicle Mass (kg)	Driving Force (N)
1.	0.19	0.16	0.27	0.00168
2.	0.19	0.13	−0.19	−0.00174
3.	0.17	0.15	−0.43	−0.00175
4.	0.18	0.16	−0.97	−0.00420
5.	0.19	0.13	−1.28	−0.01259
6.	0.22	0.15	−1.58	−0.01942
7.	0.16	0.15	−0.11	−0.00007
8.	0.17	0.15	−0.23	−0.00076
9.	0.21	0.16	−0.69	−0.00678
10.	0.16	0.15	−1.02	−0.00145
11.	0.16	0.13	−1.48	−0.00844
12.	0.17	0.16	−0.01	−0.00002
13.	0.17	0.16	−0.26	−0.00033
14.	0.18	0.17	−0.72	−0.00202
15.	0.20	0.17	−1.05	−0.00633
16.	0.23	0.19	−1.50	−0.01227

From the given table, it can be noticed that the points which highlight negative values for the effective vehicle weight ensures that there was no frictional force between the tires and the ground. That means that the vehicle was already floating. Moreover, the value attained for the rolling friction was low compared to the frictional resistance because when a tire rolls on a surface then the contact of the tire with the ground is for limited span of time. On the other hand, the frictional resistance was high

Table 7
Floating failure evaluated by comparing F_B and $W_T \cos\theta$.

No.	Water Depth, (m)	Buoyancy Force (N)	Vehicle Weight (N), $W_T \cos\theta$	($F_B > W_T \cos\theta$) – Eq. 1
1.	0.047	5.99	8.61	×
2.	0.059	10.46	8.61	✓
3.	0.065	12.79	8.61	✓
4.	0.077	18.07	8.61	✓
5.	0.083	21.02	8.61	✓
6.	0.089	23.93	8.61	✓
7.	0.057	9.70	8.61	✓
8.	0.060	10.84	8.61	✓
9.	0.071	15.35	8.61	✓
10.	0.078	18.55	8.61	✓
11.	0.087	22.97	8.61	✓
12.	0.055	8.72	8.61	✓
13.	0.061	11.23	8.61	✓
14.	0.072	15.80	8.61	✓
15.	0.079	19.05	8.61	✓
16.	0.088	23.45	8.61	✓

perpendicular to the incoming flow. Thus, it can be concluded that as the water depth around the vicinity of the vehicle increases, the capability of the tires to retain frictional resistance with the ground is reduced.

Driving force

For the estimation of the driving force, the two known distances were marked on the designed low-lying platform. The time taken by the vehicle to cross a particular point was noticed while performing the experimental runs so that the initial and final velocities of the car can be assessed to compute the vehicle acceleration. The driving force attained by the vehicle for all data points on the low-lying flooded street has been shown in Table 6.

Instability failure mode

Floating instability is witnessed when the water level reaches a critical point where the buoyancy force exceeds vehicle weight. This force always points upward in the vertical direction, thus, the pressure exerted by the fluid increases with depth and causes the vehicle to float. For the buoyancy force to take effect on a low-lying flooded roadway, the mode of floating instability relies on the same criterion as for the flat surface but due to slope inclination, the value of W_T is reduced to $W_T \cos\theta$. However, the mode of floating instability would occur when:

$$F_B > W_T \cos\theta \quad (1)$$

where, F_B is the buoyancy force and $W_T \cos\theta$ is the weight component perpendicular to the plane.

Conversely, the criterion of sliding instability differs because of different governing parameters. At inclinations, the weight component perpendicular to the plane significantly influences the frictional force which in turn affects the sliding mechanism. Basically, the weight component perpendicular to the plane reduces the net weight of the vehicle to $F_G \cos\theta$, which further effects the frictional force *i.e.* $\mu F_G \cos\theta$. On the other hand, the weight component parallel to plane supports the drag to overcome the frictional resistance, rolling friction and the driving forces which in return increases the possibility of sliding instability. Thus, the impact of drag force to cause sliding instability is increased to $F_D + F_G \sin\theta$ [23]. Therefore, the criterion of sliding instability for vehicles at inclinations can be given as:

$$F_D + F_G \sin\theta > F_{RO} + F_R + F_{DV} \quad (2)$$

where, F_D is the drag force acting at the side end of the vehicle, $F_G \sin\theta$ is the weight component parallel to the plane, F_{RO} is the rolling friction generated by tires rotation, F_R is the frictional resistance that oppose the drag impact at the side end of the vehicle and F_{DV} represents driving force of the car.

Table 8
Sliding failure assessed by comparing $F_D + F_G \sin\theta$ and F_{RO}, F_R and F_{DV}.

No.	$F_D + F_G \sin\theta$ (N)	Rolling Friction (N), F_{RO}	Friction Force (N), F_R	Driving Force (N), F_{DV}	$F_D + F_G \sin\theta > F_{Roll} + F_{Fr} + F_{Dv}$ – Eq. 2
1.	0.69	0.13	0.50	0.00168	✓

Based on the given statements, Table 7 highlights floating failure evaluated by comparing F_B and $W_T \cos\theta$. On the other hand, Table 8 highlights sliding failure assessed by comparing $F_D + F_G \sin\theta$ and F_{RO}, F_R and F_{DV}.

From the given table, it can be noticed that for any increment in the water depth, the buoyancy impact on the vehicle also increased. At points, where the buoyancy force surpassed vehicle weight, the vehicle lifted off the ground and floated away. It has been further assessed that only at one point the vehicle was found either stable or sliding which can be justified through comparison between $F_D + F_G \sin\theta$, F_{RO}, F_R and F_{DV}.

From the above table, it can be seen that below critical water depth *i.e.* low water depth, the flow velocity was sufficient enough to cause sliding failure mechanism. Thus, upon comparing the dominancy of hydrodynamic forces on the non-static vehicle as highlighted in Tables 7 and 8, respectively, with the laboratory investigations performed as shown in Fig. 3, a very good agreement between the two can be noticed.

Conclusions

The main findings of the study have highlighted that: (i) under partial submergence, lower depths were required at high flows, whereas at higher depths low flow velocities were sufficient to cause sliding instability, (ii) frictional resistance of the tires with the ground surface reduced due to perpendicular component of the gravitational force, (iii) the weight component parallel to plane assisted drag force to cause sliding mechanism and lastly (iv) the critical water depth to cause floating instability was noticed when water depth was greater than and equal to 0.055 m. The observations made through experimental investigations agreed well with the data points attained through theoretical assessment. Thus, it can be said that the study outcomes provide a preliminary criterion of hazard level for the vehicles moving on the low-lying flooded roadways.

Conflict of interest

The authors have declared no conflict of interest.

Acknowledgement

This research was supported by Universiti Teknologi PETRONAS (UTP) Internal Grant (URIF 0153AAG24), the prototype fund grant (Cost Center: 015PBA – 008) and the Technology Innovation Program (Grant No.: 10053121) funded by the Ministry of Trade, Industry and Energy (MI, Korea).

References

[1] D. Henstra, et al., Flood risk management and shared responsibility: exploring Canadian public attitudes and expectations, J. Flood Risk Manag. 12 (1) (2019) e12346.
[2] M. Pearson, K. Hamilton, Investigating driver willingness to drive through flooded waterways, Accid. Anal. Prev. 72 (2014) 382–390.
[3] M. Diakakis, G. Deligiannakis, Flood fatalities in Greece: 1970–2010, J. Flood Risk Manag. 10 (1) (2017) 115–123.
[4] P.-H. Bazin, et al., Influence of detailed topography when modeling flows in street junction during urban flood, J. Disaster Res. 7 (2012) 560–566.
[5] S. Starita, M.P. Scaparra, J.R. O'Hanley, A dynamic model for road protection against flooding, J. Oper. Res. Soc. 68 (1) (2017) 74–88.

[6] C. Arrighi, et al., Preparedness against mobility disruption by floods, Sci. Total Environ. 654 (2019) 1010–1022.
[7] Smith, G.P., B.D. Modra, and S. Felder, Full-scale testing of stability curves for vehicles in flood waters. J. Flood Risk Manag.. 0(0): p. e12527.
[8] A. Gissing, et al., Influence of road characteristics on flood fatalities in Australia, Environ. Hazards (2019) 1–12.
[9] K. Hamilton, et al., Driving through floodwater: exploring driver decisions through the lived experience, Int. J. Disas. Risk Reduct. 34 (2019) 346–355.
[10] K. Pyatkova, et al., Flood impacts on road transportation using microscopic traffic modelling techniques, in: Simulating Urban Traffic Scenarios, Springer, 2019, pp. 115–126.
[11] J.J. Keech, et al., The lived experience of rescuing people who have driven into floodwater: understanding challenges and identifying areas for providing support, Health Promot. J. Aust. 30 (2) (2019) 252–257.
[12] S.D. Drobot, C. Benight, E. Gruntfest, Risk factors for driving into flooded roads, Environ. Hazards 7 (3) (2007) 227–234.
[13] F.Y. Teo, et al., Investigations of hazard risks relating to vehicles moving in flood, J. Water Resour. Manag. 1 (1) (2012) 52–66.
[14] M. Kramer, K. Terheiden, S. Wieprecht, Safety criteria for the trafficability of inundated roads in urban floodings, Int. J. Disas. Risk Reduct. 17 (2016) 77–84.
[15] M.R.f.B.a.N.H. CRCA. Gissing, S. Opper, J. Van Leeuwen (Eds.), Influence of Road Characteristics on Flood Rescues in Australia, 2018.
[16] A. Bonham, R.T. Hattersley, Low Level Causeways, 1967.
[17] A. Gordon, P. Stone, Car Stability on Road Floodways, National Capital Development Commission, 1973.
[18] R.J. Keller, B. Mitsch, Safety Aspects of the Design of Roadways as Floodways, Urban Water Research Association of Australia, Melbourne, Australia, 1993.
[19] F.Y. Teo, et al., Experimental studies on the interaction between vehicles and floodplain flows, Int. J. River Basin Manag. 10 (2) (2012) 149–160.
[20] J. Xia, et al., Formula of incipient velocity for flooded vehicles, Nat. Hazards 58 (1) (2011) 1–14.
[21] C. Shu, et al., Incipient velocity for partially submerged vehicles in floodwaters, J. Hydraul. Res. 49 (6) (2011) 709–717.
[22] K. Toda, T. Ishigaki, T. Ozaki, Experimental study on floating cars in flood water, in: International Conference on Flood Resilience: Experiences in Asia and Europe, 2013.
[23] J. Xia, et al., Criterion of vehicle stability in floodwaters based on theoretical and experimental studies, Nat. Hazards 70 (2) (2013) 1619–1630.
[24] E. Martínez-Gomariz, et al., A new experiments-based methodology to define the stability threshold for any vehicle exposed to flooding, Urban Water J. (2017) 1–10.
[25] S.M.H. Shah, et al., Influence of forces on vehicle's instability in floodwaters, Ain Shams Eng. J. 9 (4) (2018) 3245–3258.
[26] S.M.H. Shah, Z. Mustaffa, K.W. Yusof, Experimental studies on the threshold of vehicle instability in floodwaters, Jurnal Teknologi 80 (5) (2018) 25–36.
[27] P.M. Gerhart, R.J. Gross, Fundamentals of Fluid Mechanics, Addison-Wesley, 1985.